Mine Water and the Environment (2018) 37:442–455
https://doi.org/10.1007/s10230-018-0517-1

TECHNICAL ARTICLE

Surface Water Control for Mining Thick, Relatively Shallow Coal Seams in the Loess Area of Western China

Ge Zhu[1] · Xiong Wu[1] · Shan Yu[2] · Cheng Qian[1] · Yanyan Dong[1] · Chaojun Zhang[1] · Chu Wu[1]

Received: 25 October 2016 / Accepted: 5 June 2017 / Published online: 14 February 2018

Abstract

Disastrous surface water incursions can easily occur during mining in the loess area of western China because of the shallow depth and great thickness of the coal seams there. Effective water control and drainage measures are essential to prevent such disasters. Using panels 90102 and 90103 of the Antaibao Mine of the Pingshuo mining area, Shanxi Province, as a case study, we analyzed the causes of the problem and the risk of surface water infiltration. Based on the vertical zoning features of the predicted deformation of the overburden strata and ground movement, the water-conductive fracture zone was 149.7 m thick, which means that mining could induce the inrush of surface water into the mining areas. A comprehensive set of methods was proposed, including excavation of drainage ditches, backfilling of subsiding areas, and construction of underground drainage channels. While these modifications were made in response to the geological and topographical conditions and surface drainage patterns of this site, similar methods can be used for other mines in loess areas.

Keywords Mining area · Shallow burial depth and large thickness · Surface water disaster · Prevention and control measures

Introduction

The coal mining industry is an important pillar of China's national economy (Zhang 2005; Zhang and Peng 2005; Zhang and Shen 2004). However, because of complex geological and hydrogeological conditions, various types of coal mine water disasters occur in China that seriously threaten the safety of the work and cause huge human and economic losses (Bai 2009; Wu et al. 2016a; Wu et al. 2014a, b). The four main water disaster types in China are high-pressure confined karst water inrush through the coal seam floor, water inrush through the roof from unconsolidated sandstone layers, water disasters from abandoned coal pits and old mine goafs, and infiltration of surface water and quaternary groundwater (Dong and Hu 2007; Hu and Tian 2010; Wu et al. 2013). Chinese researchers have systematically studied these disasters, including the nature of aquifer deformation and the failure mechanisms of overlying and underlying coal seams (Zhao et al. 2016), the risk assessment and zoning of coal mine water disasters (Li et al. 2014; Wu et al. 2016b), and ways to prevent water disasters (Aguado and Nicieza 2007; Chen et al. 2013a, b).

Previous studies have mostly been concerned with the first three types of water disasters, but there have been few studies on water disasters caused by surface water infiltration (Zhu et al. 2014). Western China, including Inner Mongolia, Shanxi Province, and Gansu Province, is an important coal energy production area. The topography and landforms of the Loess Plateau in western China are complex, with massive hills and gullies. The coal seams in this area are usually thick and relatively close to the surface, so mining can quite easily cause deep, wide fissures and obvious subsidence areas, especially in the gully regions (Wu and Wang 2006). The strata overlying the coal seams are seriously disturbed and damaged by the mining process. As a result, surface runoff can flow through the fissures into the mine and cause surface water infiltration disasters (Chen et al. 2016; Sun et al. 2012, 2015). We focused on panel 90102–90103 of the Antaibao No. 3 underground coal mine in the Pingshuo

✉ Ge Zhu
zhuanzhuge729@163.com

[1] School of Water Resources and Environment, China University of Geosciences, Beijing, NO. 29 Xueyuan Road, Beijing 100083, China

[2] National School, Beijing Vocational College of Labour and Social Security, NO. 5 Huixindong Street, Beijing 100082, China

mining region, Shanxi Province, as a case study on how to anticipate and prevent water disasters caused by surface water infiltration. The measures taken can be a useful reference for other mines threatened by surface water disasters in similar loess areas in western China.

The Study Area

The Antaibao No. 3 underground coal mine is one of the main coal mines of China Coal Pingshuo Group Co., Ltd., with a production capacity of 15 million t/a. The Pingshuo mine area is in the north of the Ningwu coal field, Shanxi Province. The coal mine land area is 275 km^2, with proven coal geological reserves of over 9.1 billion t. The Pingshuo mine area is one of the main coal production bases in China and comprises three super large open pits (the Antaibao, Anjialing, and East pits), each with a production capacity of 20 million t/a, and three modern underground coal mines (the Antaibao No. 3, Anjialing No. 1, and Anjialing No. 2 mines), each with a production capacity of 15 million t/a. The locations of these coal mines are shown in Fig. 1.

The Antaibao No. 3 underground mine is located in Jingping, Pinglu District, and is only 28 km from downtown Shuozhou City. The study area is located in the southwestern part of the mine, between latitudes 39°32′38″–39°35′26″N and longitudes 112°18′55″–112°24′03″E. The whole mine is 7303 m in length (EW) and 3466 m in width (NS). Panel 90102–90103 is in the southwest portion of the mine and has an area of 0.765 km^2.

The mine area belongs to a continental climate that is dry, cold, very windy, and dusty. The temperature is relatively low, with great day–night temperature differences. The average annual precipitation in the last three decades was 426.7 mm. Approximately 75–90% of the annual rainfall occurs from July to September and the average annual evaporation is 2006.7 mm.

Topographically, the terrain undulates, with an overall trend of topographic highs to lows from east to west, with altitudes of 1450–1355 m. The gentle slope angle is

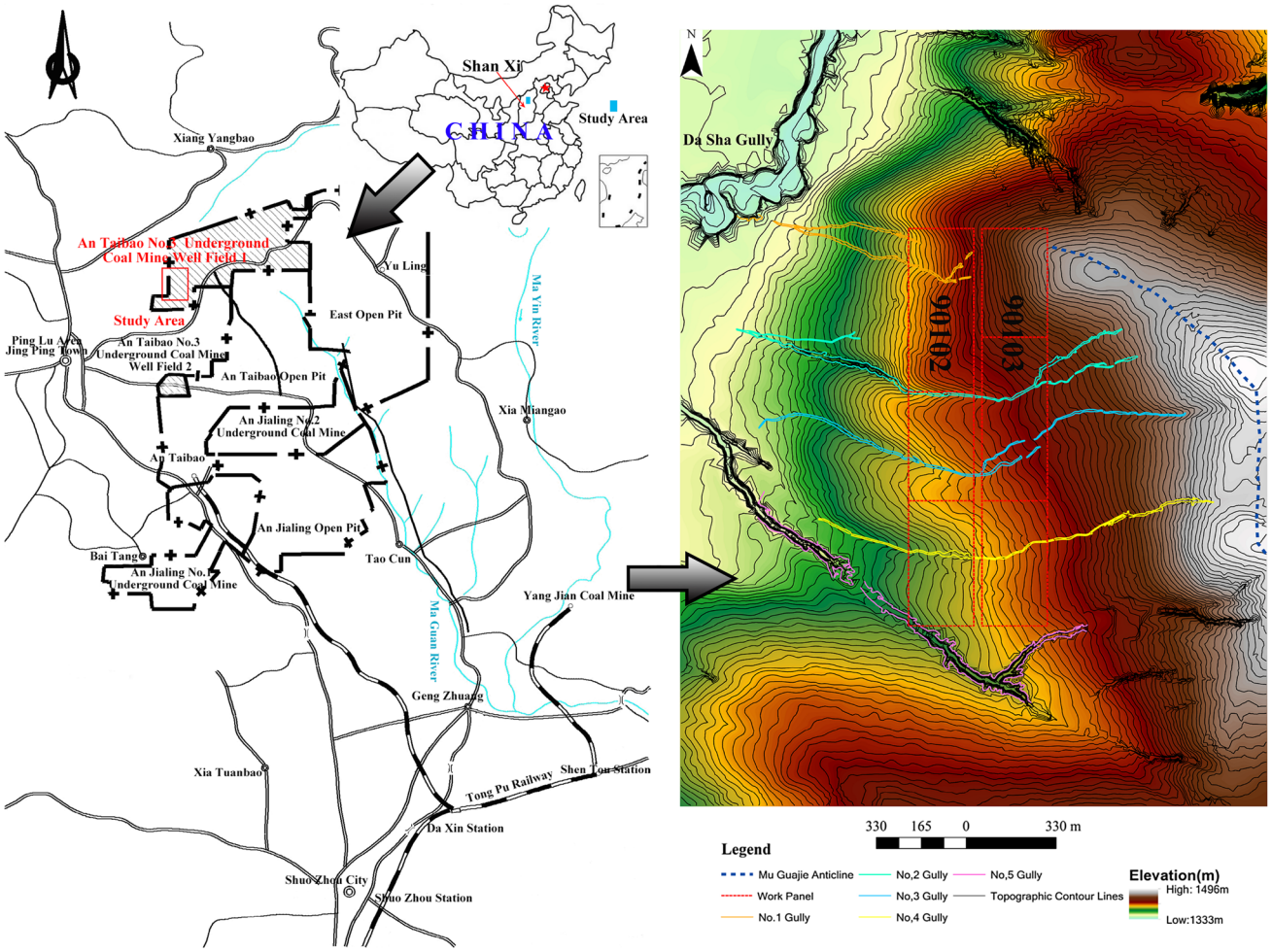

Fig. 1 Location and original topography of study area

Fig. 2 Typical loess gully landform in study area

approximately 3°–10°. The Cenozoic loess covers most of the region, with little vegetation. Strong erosion has created the typical Loess Plateau geomorphological units: loess hills (mao), loess ridges (liang), and the loess tableland (yuan). The valleys and gullies develop with a dendritic distribution and display V- and U-shapes with incised depths up to 30–50 m. Based on these features, we consider the study area to be a typical loess hilly region (Fig. 2).

Panel 90102–90103 lies on the west side of the top of a loess hill with the Dasha Gully on its northwest and the Muguajie Anticline on its east. There are five gullies near the workface, which were numbered 1–5 from north to south (Fig. 1). The first four gullies cross over the panel from east to west, and all four have a rough bottom and steep slopes on both sides. They are all small, only 1–3 m deep and 2–4 m wide. The No. 5 Gully is significantly larger and located just south of the work panel. It is from 5 to 10 m deep, and 10–15 m wide.

The mine area is mostly covered by Cenozoic strata, which include, from old to new: the Ordovician (O_2–O_3), the Upper Carboniferous (C_2), the Permian (P), the Neogene (N), and the Quaternary Pleistocene and Holocene (Q_1, Q_2). The coal-bearing strata are within the Upper Carboniferous and the Lower Permian (C_2–P_1) Taiyuan Formation (Wang et al. 2014). In the Antaibao Mine, the 9th coal seam, which has a gentle inclination, is the main minable layer, with an average thickness of 11.82 m. The geological structure of the site is simple. Panel 90102–90103 is located on the south flank of the Muguajie Anticline, and there are four faults developed in this area, with fault throws of less than 4 m (Fig. 3).

The overlying aquifers are the coal measure strata and the Quaternary phreatic aquifers. The water yield of the coal measure strata is medium–weak. The Quaternary phreatic aquifers include the loess aquifer and the alluvial or alluvial-diluvial sand-gravel aquifer that lies in the Dashagou valley region, west of the mining area. The loess aquifer is

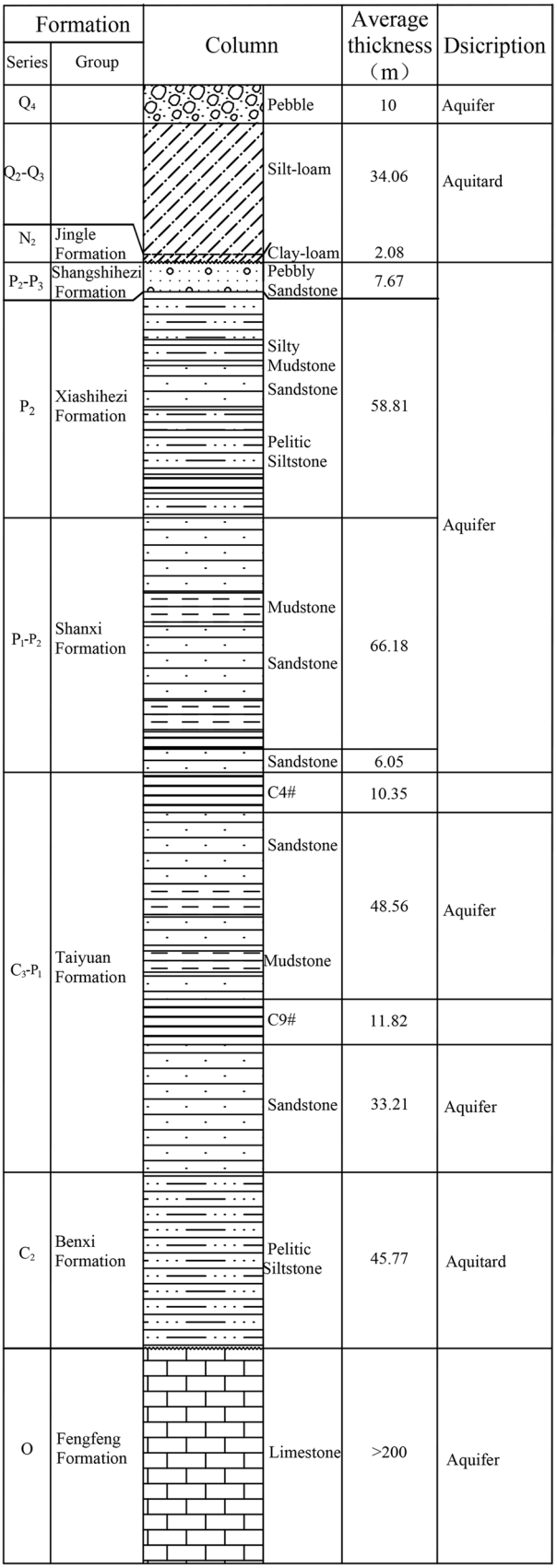

Fig. 3 Histogram of the floor strata of the study area

characterized by vertical joints, macro-pores, and phreatic water; therefore, the aquifer has a weak water yield but high permeability. The sandy gravel aquifer, mostly recharged by atmospheric precipitation, has a high water yield and a thickness of 13–30 m. Mudstone and sandy mudstone overlying the coal seam between the sandstone of the Permian and Carboniferous systems form an aquitard, but the red clay aquiclude of the Neogene System Jingle Formation is missing in this area. Consequently, surface water and Quaternary aquifer groundwater can quite easily infiltrate during mining activities.

Methods

Water-Conductive Fractured Zone Calculation

Equations (1) and (2) were used to calculate the height of the water-conductive fracture zones in the overlying strata in this study, as recommended by the "Rules for the mine extraction and coal pillars establishment under buildings, water bodies, railways and main laneways" (China National Bureau of Coal Industry 2000, hereinafter referred to as "Three Undering").

$$H_{li} = \frac{100\sum M}{1.6\sum M + 3.6} \pm 5.6, \quad (1)$$

$$H_{li} = 20\sqrt{\sum M} + 10. \quad (2)$$

H_{li} represents the height of the water-conductive fracture zone and M represents the thickness of the coal seam. For security considerations, the greater calculated result of the two formulas was chosen for the evaluation (Yao et al. 2012). The result showed that when the 9th coal seam is mined, the height of the water-conductive fracture zone could be as high as 78.8 m. Moreover, it is important to note that the empirical formulas assumes the use of longwall mining as a precondition, while panel 90102–90103 uses the top coal caving mining method. Much engineering practice and on-site experience in the Pingshuo Mine has demonstrated that the top coal caving method results in a larger water-conductive fracture zone than longwall mining (Xu et al. 2011).

The "Three Undering" stipulates that the thickness of the water-proof protective coal pillar should be six times as thick as the coal seam, so the thickness of the protective coal pillar of the 9th coal seam should be 70.9 m (Shu et al. 2016; Yang and Teng 2009) and the total thickness of the water-conductive fracture zone and protective layer should be 149.7 m (Fang et al. 2016).

Ground Movement and Deformation Forecast

When a coal seam is mined out, the overlying strata's stress balance is destroyed, so the inner stresses of the rock mass will be redistributed. This process will cause the nearby rock mass to undergo stope failure and ultimately surface collapse as mining progresses. This study combined the probability integral method and the numerical modeling recommended by "Three Undering" to forecast the extent of surface collapse (Zhang et al. 2016).

Panels 90102 and 90103 were planned to be mined in six steps, and each step was calculated as being in the rainy or dry seasons, assuming a mining speed of 200 m per month (Li et al. 2010). Steps 1, 2, and 3 occurred in panel 90102 and steps 4, 5, and 6 in 90103. Combining each step's calculated result, values for the surface horizontal displacement, subsidence, incline, and collapse boundary angle scope were obtained (Table 1).

FLAC^{3D} Numerical Modeling

To elucidate the failure of the overlying strata, the explicit three-dimensional finite difference program FLAC3D (Fast Lagrangian Analysis of Continua, Version 3.0, ITASCA, America) was used for numerical modeling (Akbarzadeh and Chalaturnyk 2014; Wu et al. 2006). The western boundary extended 1000 m from the western margin of panel 90102, and the eastern, northern, and southern boundaries extended 1000 m from the eastern, northern, and southern margins of the panel, respectively. The bottom margin extended 300 m from the maximum burial depth of the coal seam. The width direction (east–west) was the X axis, the length direction

Table 1 Surface deformation forecasting result (probability integral method)

Step	Work face	Max horizontal displacement (m)	Max subsidence value (m)	Max incline	Max collapse boundary angle scope (m)
1	90102 first step	2.87299	9.54	0.25135	91.3
2	90102 second step	2.87298	9.56	0.251	92.6
3	90102 third step	2.87299	9.57	0.25136	93.5
4	90103 first step	2.87299	9.52	0.25135	92.2
5	90103 second step	2.87298	9.57	0.25136	93.6
6	90103 third step	2.87299	9.58	0.25023	94.5

(north–south) was the Y axis, and the vertical direction along the buried coal seam was the Z axis (Wang et al. 2014; Wu et al. 2007). The Taiyuan Formation was divided into five layers: the stratum overlying the 4th coal seam, the 4th coal seam (including the interlayer between 4-1 and 4-2), the stratum between the 4th and 9th coal seams, the 9th coal seam, and the stratum between the 9th coal seam and the Ordovician top boundary. The whole model was meshed into 232,368 hexahedral zones and 254,085 grids (Fig. 4; Kang et al. 2014).

Following the Mohr–Coulomb constitutive relation and considering the faults as entity units, an elastic–plastic model was established. The calculation boundary was constrained in displacement, the X and Y axes were constrained in normal displacement, and the bottom was multi-constrained. The calculation parameters were ascertained by laboratory tests and engineering analogy methods (Table 2), according to the physical and mechanical parameters of the strata in the study area given by the Anjialing Coal Mine Geology Report (Shanxi Province 115 Coal Geological Exploration Industry 2001), using data from the Pingshuo mine.

The mining was also divided into six steps like the probability integral method (Table 3; Fig. 5). There is little difference between the predicted results of the two methods. For safety considerations, the larger values were chosen for the engineering design.

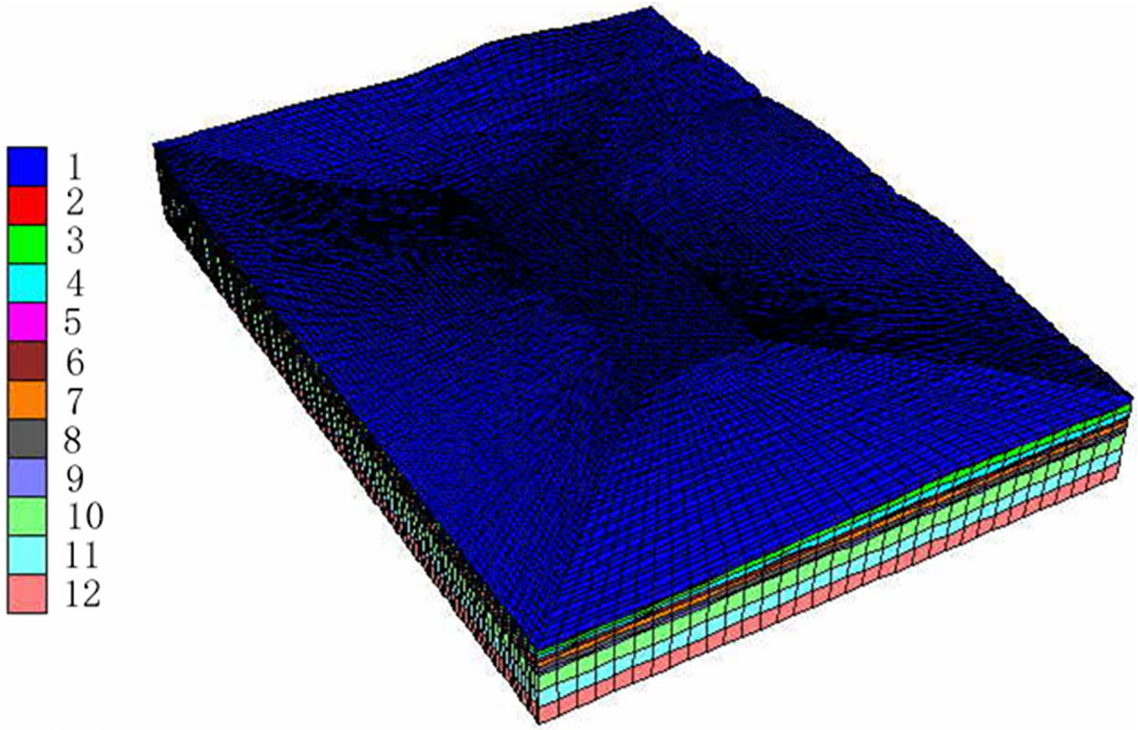

Fig. 4 FLAC3D numerical model

Table 2 Calculation parameters

Strata	elasticity modulus (MPa)	Poisson's ratio	Unit weight (KN/m^3)	Internal friction angle (°)	Adhesive aggregation (MPa)
O_2	16,000	0.27	2700	42	1.2
C_{2+3}	7500	0.29	2650	35	1.0
P_1X	3500	0.27	2650	35	0.6
P_1S	3300	0.27	2650	33	0.4
P_2S	4000	0.28	2640	32	0.45
N_2b	3500	0.27	2600	32	0.5
Q_{2+3}	1000	0.36	2000	22	0.4
Coal seam	2350	0.33	2350	25	0.1

Table 3 Surface deformation forecasting result (FLAC^{3D} numerical modeling method)

Mining steps	Mining coal seams	Max. subsidence (m)	Collapse scope (m)
1	90102 first step	9.48	98.2
2	90102 second step	9.65	100.3
3	90102 third step	9.76	102.5
4	90103 first step	9.32	97.5
5	90103 second step	9.7	104.2
6	90103 third step	9.72	101.6

Results

The 9th coal seam is 70–180 m below the surface (Fig. 6). The calculated results of the water-conductive fracture zone show that some transmission fissure zones can reach the surface in the study area, especially in the gullied regions. Therefore, surface water can quite easily rush into the mine (Wu et al. 2015). In addition, the Neogene System Jingle Formation is missing in the study area, so the unconsolidated Quaternary Upper Pleistocene formation lies directly on the sandstone that overlies the 9th coal seam and has a close hydraulic relation to it. Even in regions where the fissured zone does not connect to the surface, the surface water still has a high probability of rushing into the mine through the aquifer overlying the coal seam (Krzysztof et al. 2016). The contour in Fig. 7 represents the thickness of the coal seam burial depth minus the water-conductive fractured zone development height. The yellow part of the figure reveals where the fissure directly connects to the surface and the orange part represents the thickness of the protective layer, which is greater than 0 but less than six times the thickness of the coal seam (Sun et al. 2015a, b).

According to "Three Undering," and practical experience elsewhere in the Pingshuo Mine, large, deep fissures will certainly form. Exploration results revealed that the fissures that developed were over 10 m deep and reached the transmission fissure zones (Wang and Jia 2003). When the 9th coal seam is mined, the surface will undergo serious collapse. This may change the original topography and landform, resulting in changes to the surface runoff and insufficient water flow, especially in

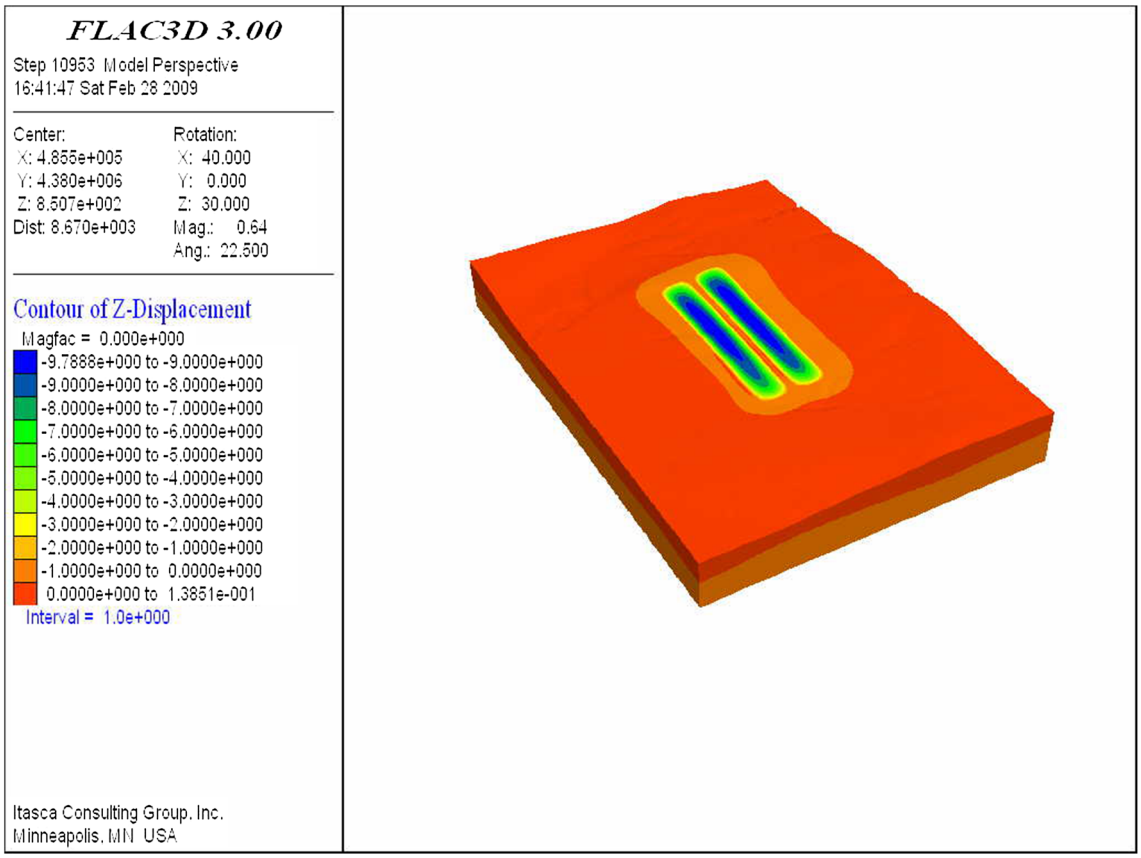

Fig. 5 Cloud chart of ground deformation forecast after mining

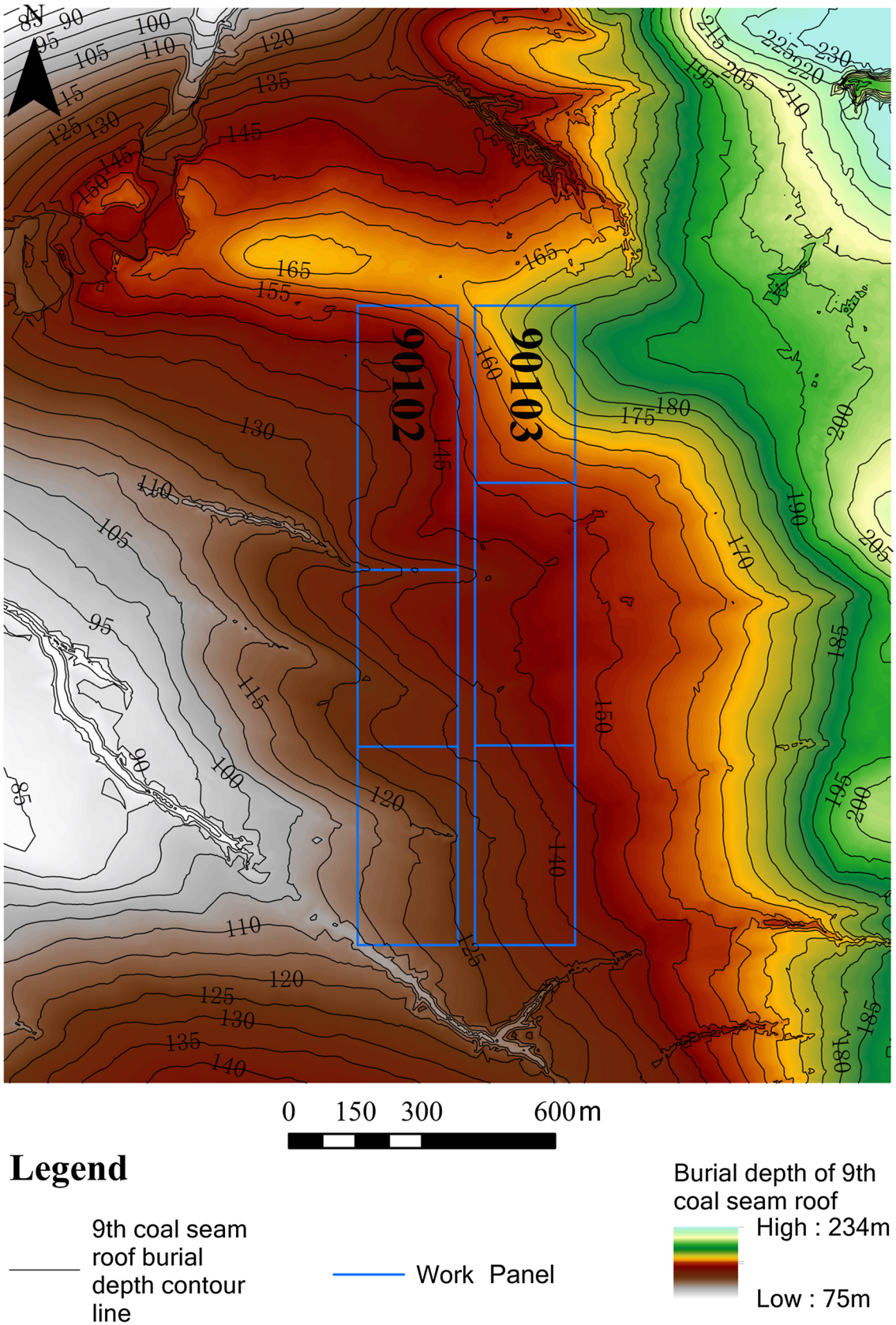

Fig. 6 Burial depth of the 9th coal seam roof

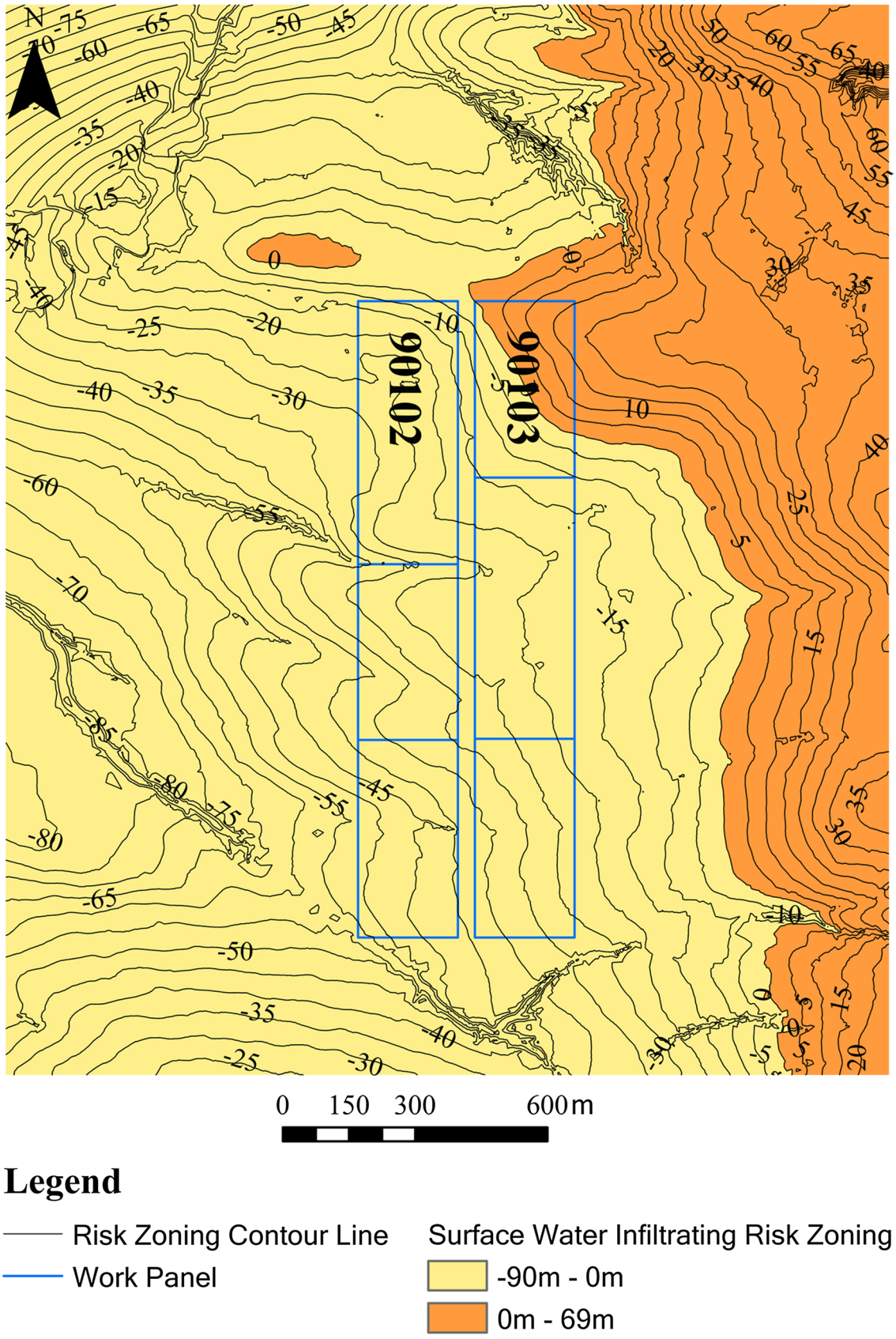

Fig. 7 Surface water infiltrating risk zoning

some gullied areas (Wu et al. 2011). Furthermore, the intensive rainfall in the study area can easily cause large-scale surface runoff during the rainy season to a degree that cannot easily be dissipated by normal flow processes, causing more surface water to rush into the mine.

Discussion

Work Panel Deformation After Mining

Figure 8a shows a topographic map of panel 90102 after the first mining step. The map shows that there are two subsidence areas near the No. 1 gully in the north of the panel. The subsidence areas are approximately 4 m deep and can lead to the formation of ponding on the surface. During step 1, the topography was changed little by mining in the other influenced regions, but the whole topography remained higher in the east and lower in the west with a 4° slope, which made it impossible for surface water to gather. Figure 8b shows a topographic map of panel 90102 after the second mining step. It is clear that two additional subsidence areas with depths of 6–8 m have formed over in the No. 2 and 3 Gullies. The whole topography has not changed much, with the western area lower and the eastern area higher, and the surface water is still unable to gather on the slope surface. Figure 8c is a topographic map of panel 90102 after the third mining step. The map shows that there is a 4 m deep subsidence area in the No. 4 Gully in the south of the work panel, but the rest of the mining-influenced region is still stable, with no trend of surface water gathering on the slope.

Figure 8d, e are topographic maps of work panel 90103 after the first and second mining steps, respectively, and reveal that the topography still allows water to flow smoothly from east to west without any obvious subsidence areas or surface ponding. Figure 8f is a topographic map of work panel #90103 after the third mining step. The picture shows a small subsidence area in the No. 4 Gully, with a depth less than 5 m. The topography in the rest of the mining-influenced area remains stable, with no possibility of surface ponding.

To sum up, mining of panels 90102 and 90103 caused some subsidence areas to develop in the gullies, slowing the flow speed and leading to surface water accumulation. However, the scale of seepage was relatively small, the topography of the entire study area remained unchanged, and the flow of the surface water in the original gullies barely changed, so the study takes advantage of the original topography to prevent and drain the surface water.

Surface Water Prevention Overall Control Principle

For the sake of mine safety, the surface water disaster prevention and drainage process should be based on four principles: (1) intercepting the peripheral water outside the working face; (2) guaranteeing the smooth flow of water in the work panel area, especially in the gullies; (3) filling the predicted subsidence areas with soils from nearby during mining to avoid surface water ponding; and (4) considering surface water infiltration when designing mine drainage projects (Zhang et al. 2013).

Drainage Ditch Arrangement

Based on these principles, two drainage ditches were dug outside of the mining influenced area before panel 90102 was mined. The two ditches were numbered Drainage Ditches 1 and 3 and lay to the south and east of panel 90102. Part of the No. 5 gully was changed so that it flowed into Drainage Ditch 3. Before panel 90103 was mined, Drainage Ditch 2 was dug east of it. Drainage Ditches 2 and 3 will remain drainage ditches, while Drainage Ditch 1 was filled up before panel 90103 was mined, after panel 90102 had been mined (Fig. 9).

Filling Project Design

The principle of a fill project is to fill the predicted subsidence areas with soil to avoid surface ponding. It is important that the surface water from upstream will not be hindered. Therefore, the digging and filling areas were designed as shown in Fig. 10.

1. Use nearby soil to fill the predicted subsidence areas during the first step of the panel 90102 mining. Convey the soils from Digging Area 1 into Filling Areas 1-0 and 1-1, and dredge Gully 1 afterwards.
2. Use nearby soil to fill the predicted subsidence areas during the second step of this mining activity. Convey the soil from Digging Areas 2-0 and 2-1 into Filling Areas 2-0 and 2-1 and dredge Gullies 2 and 3 afterwards.
3. Use nearby soil to fill the predicted subsidence areas during the third step. Convey the soil from Digging Area 3 into Filling Area 3 and dredge the original gullies (Gully 4) afterwards.
4. Use nearby soil to fill the predicted subsidence areas during the third step of panel 90103 mining. Convey the soil from Digging Area 6 into Filling Area 6 and dredge the original gullies (Gully 4) afterwards. Furthermore, fill part of Gully 5 (Filling Area 7), which is east of

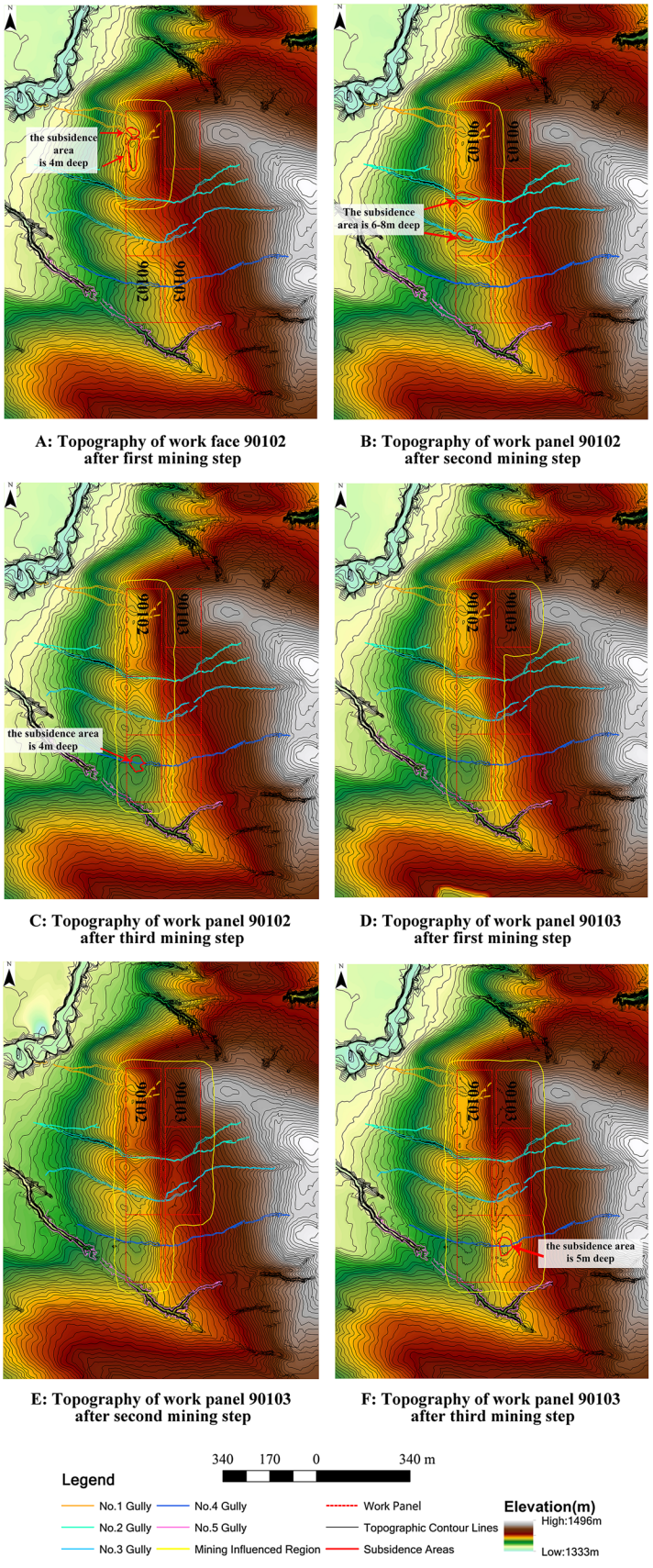

Fig. 8 Topography of work panel after mining steps

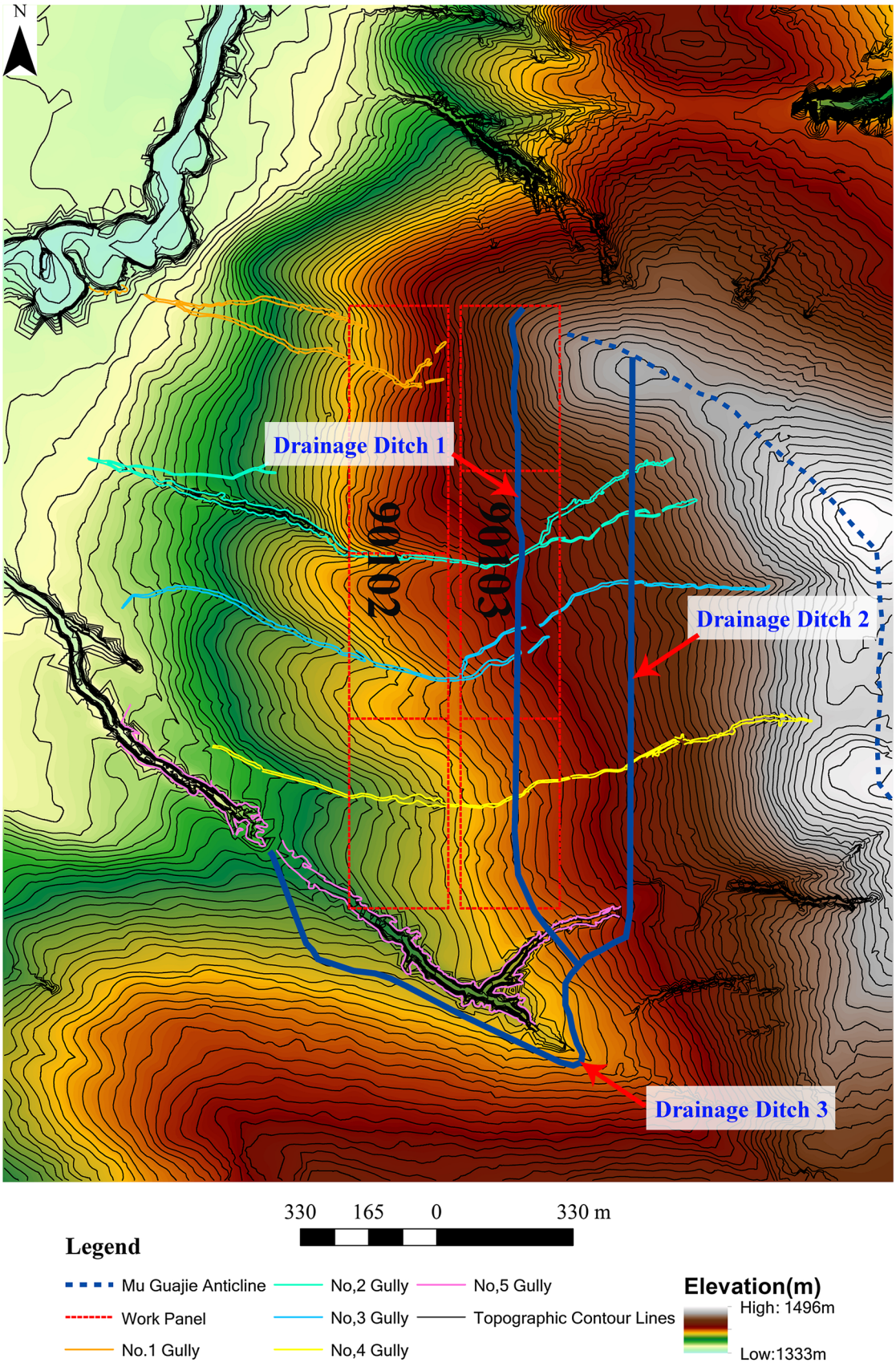

Fig. 9 Drainage ditch arrangement

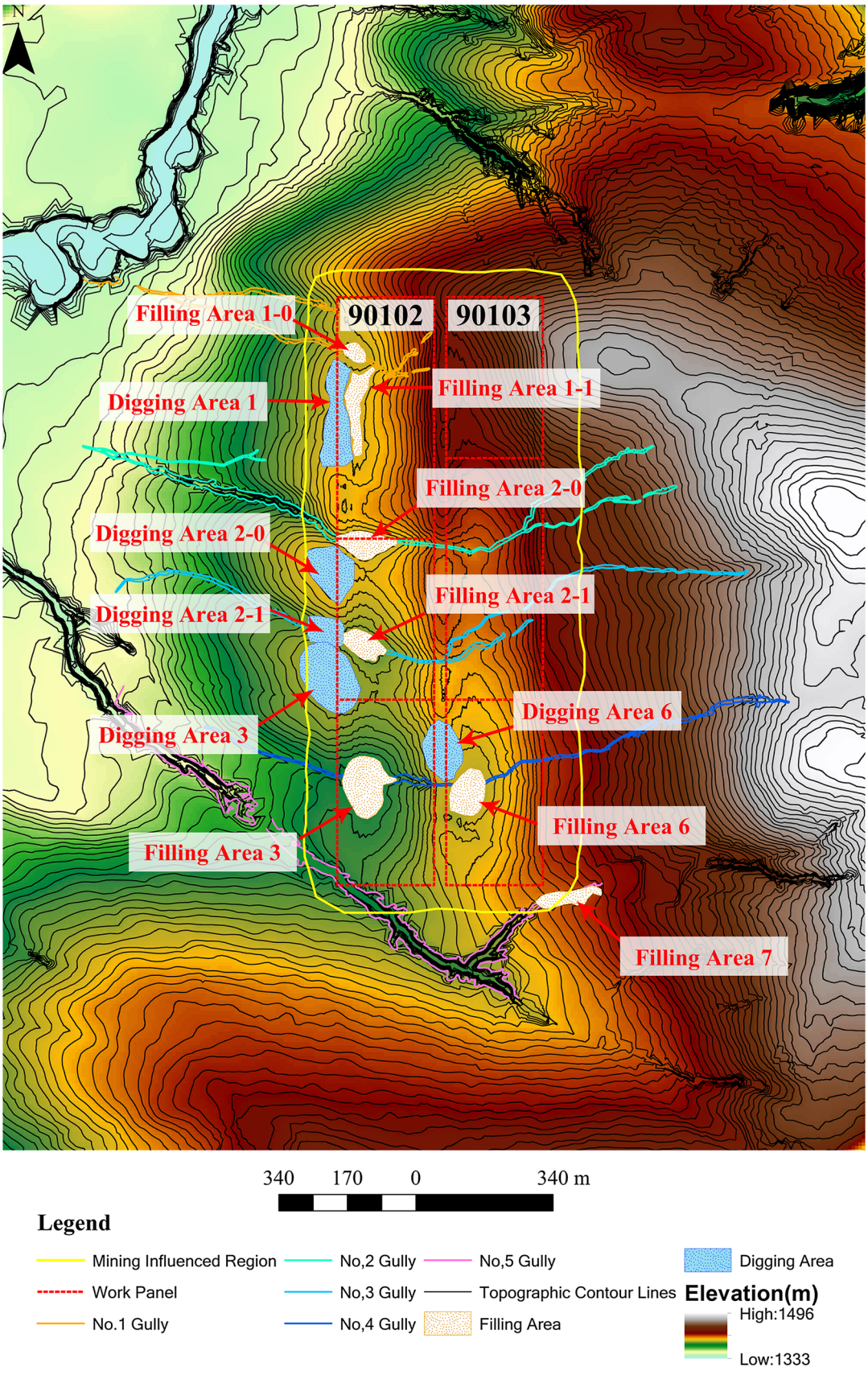

Fig. 10 Filling project during mining of work panel #90102–90103

Drainage Ditch 1, up to the surface to avoid ponding and make sure that surface water can rapidly flow away through Drainage Ditch 3.

Infiltrated Surface Water Drainage

Though measures to intercept the surface water outside the work panel and drain the surface water in the mining area have been taken, some surface water could still infiltrate into the aquifer. Given that approximately 75–90% of the average annual precipitation of 426.7 mm is received from July to September, often exceeding 100 mm per day, surface water infiltration should be taken into consideration. The surface water catchment area of panels 90102 and 90103 are 423,857 and 661,252 m^2, respectively, with an infiltration coefficient of 0.2. Based on these parameters, the quantity of water that infiltrates into the panels should total 353 and 551 m^3/h, respectively (Dong et al. 2012; He et al. 2011).

Conclusion

The Antaibao underground mine lies in a typical loess area in western China, where there are many gullies. The combination of the relatively shallow depth of the seam and the topography can quite easily cause surface water disasters during mining of the thick seam. This research represents a case study on how to address such problems. The probability integral method and FLAC3D numerical modeling were both used to forecast the surface deformation, and there was little difference between the results of the two methods. The calculated height of the water-conductive fracture zone in the study area was 149.68 m. A water-conductive fracture zone could easily develop from the coal seam to the surface, which will cause surface water to disastrously rush into the mine.

Based on the results of the probability integral method, FLAC3D numerical modeling, and the height of the water-conductive fracture zone, a comprehensive method was proposed to intercept and drain the water. Excavation and filling projects and drainage work underground were implemented. Water interception and drainage can prevent surface water from accumulating outside the mine area and can be implemented before mining even begins.

Panels 90102 and 90103 have now been completely mined. The measures suggested by our research were successful and there were no surface water disasters. This practical approach has proved to be reliable and efficient.

Acknowledgements The research was supported by the National Natural Science Foundation of China (No. 41572227), the Fundamental Research Funds for the Central Universities (No. 2652015125) and a Project supported by the Ministry of Land and Resources of China (201511056-3).

References

Akbarzadeh H, Chalaturnyk RJ (2014) Sequentially coupled flow-geomechanical modeling of underground coal gasification for a three-dimensional problem. Mitig Adapt Strateg Glob Change 21:577–594

Bai YJ (2009) Causes analysis and control technology of water disaster in coal mines. Coal Technol 28:85–87 **(in Chinese)**

Chen JJ, Chen Y, Guo WB, Zou YF (2013a) Study on surface movement law under the condition of thick unconsolidated strata. Coal Sci Technol 41:95–102 **(in Chinese)**

Chen LW, Zhang SL, Gui HR (2013b) Prevention of water and quicksand inrush during extracting contiguous coal seams under the lowermost aquifer in the unconsolidated Cenozoic alluvium—a case study. Arab J Geosci 7:2139–2149

Chen LW, Feng XQ, Xie WP, Xu DQ (2016) Prediction of water-inrush risk areas in process of mining under the unconsolidated and confined aquifer: a case study from the Qidong coal mine in China. Environ Earth Sci 75:706

Aguado MBD, Nicieza CG (2007) Control and prevention of gas outbursts in coal mines, Riosa–Olloniego coalfield, Spain. Int J Coal Geol 69:253–266

Dong SN, Hu WY (2007) Basic characteristics and main controlling factors of coal mine water hazard in China. Coal Geol Explor 35:34–37 **(in Chinese)**

Dong DL, Sun WJ, Sha X (2012) Optimization of mine drainage capacity using FEFLOW for the No. 14 coal seam of China's Linnancang coal mine. Mine Water Environ 31:353–360

Fang J, Xu HJ, Cap ZG, Li P (2016) Calculation on height of water conducted zone for fully-mechanized top coal caving mining in thick seam under soft and weak overburden strata. Coal Sci Technol 44:67–73 **(in Chinese)**

He KQ, Yu WC, Jiang WF (2011) Analysis of groundwater inrush conditions and critical inspection parameters at the Baixiangshan iron mine, China. Mine Water Environ 30:274–283

Hu WY, Tian G (2010) Mine water disaster type and prevention and control countermeasures in China. Coal Sci Technol 138:92–96 **(in Chinese)**

Kang YS, Liu QS, Gong GQ, Wang HC (2014) Application of a combined support system to the weak floor reinforcement in deep underground coal mine. Int J Rock Mech Min 71:143–150

Krzysztof P, Kazmierz R, Piotr C (2016) Causes and effects of uncontrolled water inrush into a decommissioned mine shaft. Mine Water Environ 35:128–135

Li PX, Tan ZX, Yan LL, Deng KZ (2010) Calculation method of probability integration method parameters based on support vector machine. J China Coal Soc 35:1247–1251 **(in Chinese)**

Li LP, Zhou ZQ, Li SC, Xue YG, Xu ZH, Shi SS (2014) An attribute synthetic evaluation system for risk assessment of floor water inrush in coal mines. Mine Water Environ 34:288–294

Shu ZY, Li L, Li HJ (2016) Study on conducted zone and caving zone height of overlying rock with extremely thick coal in fully-mechanized caving coal face. Coal Sci Technol 44:53–54 **(in Chinese)**

Sun WJ, Wu Q, Dong DL, Jiao J (2012) Avoiding coal–water conflicts during the development of China's large coal-producing regions. Mine Water Environ 31:74–78

Sun XQ, Jiang ZQ, Wang ZS, Li YJ (2015a) Height prediction of the "two zones" in shallow coal seam by slicing mining. Min R D 35:69–72 **(in Chinese)**

Sun WJ, Zhou WF, Jiao J (2015b) Hydrogeological classification and water inrush accidents in China's coal mines. Mine Water Environ 35:214–220

Wang YL, Jia WY (2003) Analysis and application of two zone height in deep seam mining. Coal Sci Technol 31:31–38 **(in Chinese)**

Wang ZJ, Huang ZG, Yao JX, Ma XL (2014) Characteristics and Main progress of the stratigraphic chart of China and directions. Acta Geol Sin 35:271–276 **(in Chinese)**

Wu Q, Wang MY (2006) Characterization of water bursting and discharge into underground mines with multilayered groundwater flow systems in the North China coal basin. Hydrogeol J 14:882–893

Wu X, Yu QC, Wang XG, Duan QW, Li XQ, Yang J, Bao YF (2006) Exploitation of coal resources under a surface water body. Chin J Rock Mech Eng 25:1029–1036 **(in Chinese)**

Wu X, Wang XG, Duan QW, Sun YD, Jia ZX, Li XQ (2007) Study on coal mining in seam under large reservoir areas. J China Coal Soc 32:1273–1276 **(in Chinese)**

Wu Q, Liu YZ, Yang L (2011) Using the Vulnerable index method to assess the likelihood of a water inrush through the floor of a multi-seam coal mine in China. Mine Water Environ 30:54–60

Wu Q, Cui FP, Zhao SQ, Liu SQ, Zeng YF, Gu YW (2013) Type classification and main characteristics of mine water disasters. J China Coal Soc 38:561–565 **(in Chinese)**

Wu Q, Fan ZL, Zhang ZW, Zhou WF (2014a) Evaluation and zoning of groundwater hazards in Pingshuo No. 1 underground coal mine, Shanxi Province, China. Hydrogeol J 22:1693–1705

Wu Q, Liu YZ, Zhou WF, Li BY, Zhao B, Liu SQ, Sun WJ, Zeng YF (2014b) Evaluation of water inrush vulnerability from aquifers overlying coal seams in the Menkeqing coal mine, China. Mine Water Environ 34:258–269

Wu Q, Liu YZ, Luo LH, Liu SQ, Sun WJ, Zeng YF (2015) Quantitative evaluation and prediction of water inrush vulnerability from aquifers overlying coal seams in Donghuantuo coal mine, China. Environ Earth Sci 74:1429–1437

Wu Q, Liu YZ, Wu XL, Liu SQ, Sun WJ, Zeng YF (2016a) Assessment of groundwater inrush from underlying aquifers in Tunbai coal mine, Shanxi province, China. Environ Earth Sci 75:737

Wu Q, Li B, Chen YL (2016b) Vulnerability assessment of groundwater inrush from underlying aquifers based on variable weight model and its application. Water Resour Manag 30:3331–3345

Xu YC, Li JC, Liu SQ, Zhou L (2011) Caculation on formula of "two zone" height of over lying strata and its adaptability analysis. Coal Min Technol 16:4–11 **(in Chinese)**

Yang JL, Teng YH (2009) Study on development law of water conducted fracture zone in top coal of fully mechanized top coal caving mining face. Coal Sci Technol 37:100–102 **(in Chinese)**

Yao Q, Tao F, Li SL, Li SL, Ning QY (2012) The subsidence prediction of coal mine "three under" mining based on probability integral method. Saf Coal Min 43:188–193 **(in Chinese)**

Zhang JC (2005) Investigations of water inrushes from aquifers under coal seams. Int J Rock Mech Min 42:350–360

Zhang JC, Peng SP (2005) Water inrush and environmental impact of shallow seam mining. Environ Geol 48:1068–1076

Zhang JC, Shen BH (2004) Coal mining under aquifers in China: a case study. Int J Rock Mech Min 41:629–639

Zhang ZL, Gao YF, Wu Q, Wei SM (2013) Discussion on the technical system of solid prevention and control on mining flooding. J China Coal Soc 38:378–383 **(in Chinese)**

Zhang JC, Sun Q, Zhou N, Jiang HQ, Germain D, Abro S (2016) Research and application of roadway backfill coal mining technology in western coal mining area. Arab J Geosci 9:558

Zhao K, Xu NX, Mei G, Tian H (2016) Predicting the distribution of ground fissures and water-conducted fissures induced by coal mining: a case study. Springerplus 5:977

Zhu G, Wu X, Li PH, Qi RJ, Mu WP, Fu RZ (2014) Coalmine surface water prevention and drainage in loess area. J China Coal Soc 39:1354–1360 **(in Chinese)**